Stagnation Region Solutions of the Full Viscous Shock-Layer Equations

B.N. Srivastava,* M.J. Werle† and R.T. Davis‡
University of Cincinnati, Cincinnati, Ohio

Nomenclature

ϵ = $(\gamma-1)/2\gamma$
R_n^* = nose radius
Re_∞ = freestream Reynolds number $\rho_\infty^* U_\infty^* R_n^*/\mu_\infty^*$
Re_s = shock Reynolds number $\rho_s^* \mu_s^* R_n^*/\mu_s^*$
Re_b = defined as $\rho_\infty^* U_\infty^* R_n^*/\mu_0$
Re_F = $Re_b/\epsilon 2^{1/2}$

Superscripts and subscripts

* = dimensional quantities
∞ = freestream conditions
s = behind the shock
0 = stagnation point value

I. Introduction

THE re-entry problem continues to provide motivation for study of low Reynolds number, high Mach number blunt-body flows. This flow regime is one in which the viscous effects influence a significant portion of the total shock-layer thickness, thereby violating the classical boundary-layer approximations and requiring the use of a more comprehensive set of governing equations. The viscous shock-layer equations[1,2] represent an intermediate level of approximation between the boundary-layer and Navier-Stokes equations. Although some evidence exists that the viscous shock-layer model will suffice for re-entry-type flow problems,[3,4] there has, as yet, not been a critical assessment of the range of validity of these equations. This situation is due to the difficulties involved in solution of these equations. Although the "thin-shock-layer" version of these equations has been solved by numerous authors [5,6] only a few[1,4] have addressed the full set of equations, with none conducting an assessment of the range of validity of these equations. This is performed in the present paper through comparison with experimental stagnation point data for spherical nose shapes. Numerical solutions of the viscous shock-layer equations are obtained by combining an implicit finite-difference scheme with a relaxation technique for determining the bow shock shape.[7] The effects of thin layer approximations, wall slip, and shock slip boundary conditions are included in the analysis to establish their relative importance.

II. Governing Equations and Method of Solution

It is unnecessary to present the equations, since they are included in the papers cited.[1] The governing equations include the continuity equation, two momentum equations, and energy equations together with the equation of state and Sutherland's viscosity law to complete the system. Surface slip conditions consistent with the approximations used in the preceding set of equations are the same as those given in Ref. 1. The modified Rankine-Hugoniot relations are used to obtain the flow conditions at the shock surface. These relations are obtained using the concept of "shock slip" to represent the usual higher-order Reynolds number effects on the shock compression process (see Ref. 1 for further details).

The resulting set of viscous shock-layer equations is of the parabolic-hyperbolic type and therefore is solved with a method similar to that used for solving the boundary-layer equations,such as the method of Blottner and Flugge-Lotz.[8] The calculation of the shock shape, though, represents an elliptic effect. To account properly for the shock shape, the present method of solution adopted a relaxation technique wherein the shock slope was determined iteratively with repeated passes along the surface to solve the conservation equations. At each stage of the iteration (after each pass along the surface), a least-squares Chebyshev polynomial was used to smooth the numerically calculated shock shape over the entire range of integration in the downstream direction. This method of solution was found to work well for flow past blunt bodies, where the shock standoff distance was not small and the shock shape differed significantly from the body shape. For a detailed description of the numerical method, one is referred to Ref. 9.

III. Results and Discussion

Figure 1 presents a comparison of normalized stagnation point heating with experimental data and other theoretical results. The numerical calculations were made at a freestream Mach number M_∞ of 8.0, a wall-to-stagnation-temperature ratio of 0.25, and a total temperature of 500°R. The heat flux in Fig. 1 is normalized, with its value obtained from a boundary-layer analysis at the same test conditions. Note that the full-layer results rightfully approach unity as Reynolds number increases, in good agreement with the higher-order boundary-layer theory of Van Dyke,[10] which gives

$$q/q_{BL} \rightarrow 1 + 0.866/(Re_s)^{1/2} \qquad (1)$$

Comparison of the present full-layer results (including shock and wall slip effects) with the experimental data is seen to be good over the entire Reynolds number range. However, note should be made that the data of Ferri et al.[11] which were obtained with $M_\infty = 8$, $T_w/T_0 = 0.25$, and $T_0 = 2300$°R, were found to be higher than those predicted by any of the other analytical or experimental results. Hickman et al.[12] attributed this apparent increase to the higher stagnation temperature level of Ferri's experimental condition (2300°R) as compared to their test stagnation temperature level of 500°R. However, numerical calculations using the present model with the

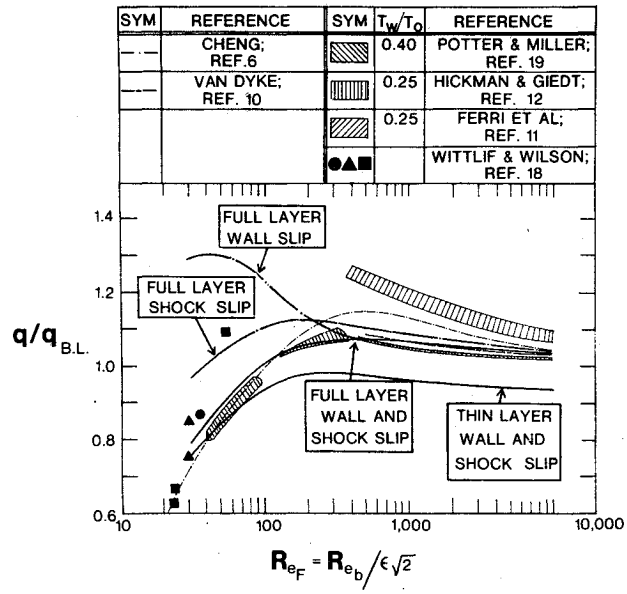

Fig. 1 Stagnation point heat transfer.

Received July 25, 1975. This research was supported by the U.S. Air Force through the Arnold Engineering Development Center under Contract F40600-74-C-0011-P00001.

Index categories: Jets, Wakes, and Viscid-Inviscid Flow Interactions; Viscous Nonboundary-Layer Flows.

*Graduate Research Assistant, Department of Aerospace Engineering.

†Professor, Department of Aerospace Engineering. Member AIAA.

‡Professor and Head, Department of Aerospace Engineering. Associate Fellow AIAA.

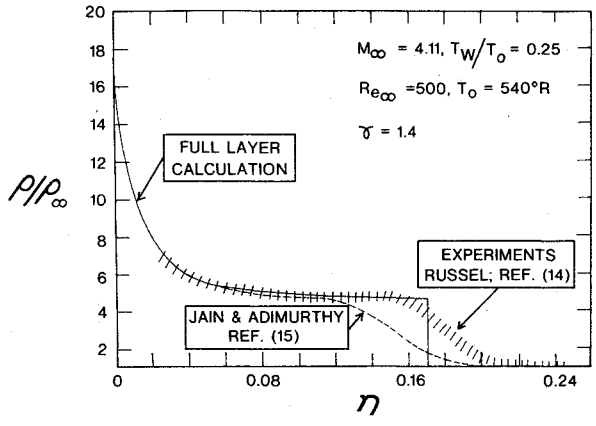

Fig. 2 Stagnation point density profile.

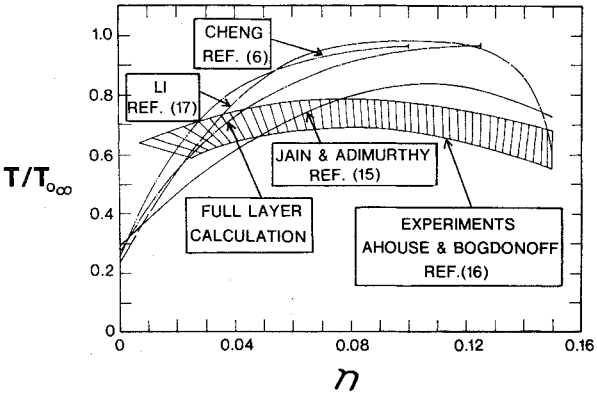

Fig. 3 Stagnation point temperature profile.

stagnation temperature corresponding to Ferri's experimental conditions do not yield results[13] as high as those obtained by Ferri et al.,[11] and this difference as yet remains unexplained.

Figure 1 also shows the analytical result of Cheng,[6] where a Newtonian thin shock layer approach was employed. Both wall and shock slip effects were incorporated in these solutions and thus are seen to compare favorably with the present calculations over the entire Reynolds number range.

In an effort to assess the importance of wall and shock slip conditions on the predicted results, solutions also were obtained without slip effects included. As shown in Fig. 1, as the Reynolds number decreases, wall slip effects become important, and then shock slip effects grow to a significant level. Both of these effects are of equal significance in the low Reynolds number regime. It thus is seen that the results predicted by the present model compare well with experimental data to very low Reynolds numbers. Similar conclusions were also made by Anderson and Moss[3] when they compared the numerical solution of these equations with numerical solution of the steady-state Navier-Stokes equations for hypersonic flow about blunt axisymmetric bodies. It is also noted from Fig. 1 that, although the full shock-layer equations yield results that compare well with various data, their thin layer approximations give results that are significantly lower than the data for the Reynolds number range shown.

In order to assess the capability of the present model to represent the full flow structure across the shock layer, comparison is made in Fig. 2 with the density profile measured by Russel[14] for flow of nitrogen past a sphere at $M_\infty = 4.11$ and shock Reynolds number Re_s of 129. The experimental result shows a finite thickness of the shock wave whose effect on the shock-layer density is seen to be modeled correctly using the shock slip approach in the present analysis. It is noted here that the shock discontinuity modeled in the present analysis rightly occurs in the middle of the shock thickness shown by the experimental data. This figure also shows the results of Jain and Adimurthy,[15] where solutions are obtained using a series truncation technique of the Navier-Stokes equations in the stagnation region. Although their results model the shock layer region well, they apparently misrepresent the shock wave region because the series truncation approach tacitly assumes the shock to be spherical over the entire stagnation region. Similar results are obtained corresponding to other test data of Russel.[13]

As a final comparison, Fig. 3 shows the temperature profile on the stagnation line of a spherical body at $M_\infty = 19$, $T_w/T_0 = 0.19$, and $Re_s = 54.0$ measured by Ahouse and Bogdonoff,[16] along with various other theoretical calculations. The results obtained by the present analysis only compare qualitatively with the experimental data, but they do show a trend similar to the shock-layer analysis of Cheng[6] and the Navier-Stokes analysis of Li.[17] Note that, even though the similarity solution of Jain and Adimurthy[15] tacitly assumes the shock to be spherical in the nose region, their results seem to be surprisingly closer to the experimental data. The exact source of the discrepancy between the present shock-layer analysis and the experimental data in the outer reaches of the layer is as yet unexplained.

In an overall sense, the results obtained here thus indicate that the viscous shock-layer model compares well with experimental data to very low Reynolds numbers. It is found that, with the inclusion of shock and body slip, the full viscous shock-layer model apparently enjoys a range of validity down to shock Reynolds numbers on the order of 20-30.

References

[1] Davis, R.T., "Numerical Solution of the Hypersonic Viscous Shock Layer Equations," *AIAA Journal*, Vol. 8, May 1970, pp. 843-851.

[2] Davis, R.T., "Hypersonic Flow of a Chemically Reacting Binary Mixture Past a Blunt Body," AIAA Paper 70-805, Los Angeles, Calif. 1970.

[3] Anderson, E.C. and Moss, J.N., "Numerical Solution of the Steady-State Navier-Strokes Equations for Hypersonic Flow About Blunt Axisymmetric Bodies," TMX-71977, 1973, NASA.

[4] Miner, E.W. and Lewis, C.H., "Hypersonic Ionizing Air Viscous Shock-Layer Flows Over Sphere Cones," *AIAA Journal*, Vol. 13, Jan. 1975, pp. 80-88.

[5] Dellinger, T.C., "Nonequilibrium Air Ionisation in Hypersonic Fully Viscous Shock Layers," AIAA Paper 70-806, Los Angeles, Calif., 1970.

[6] Cheng, H.K., "The Blunt-Body Problem in Hypersonic Flow at Low Reynolds Number," Rept. AF-1285-A-10, 1963, Cornell Aeronautical Laboratory, Buffalo, N.Y.

[7] Davis, R.T. and Nei, Y.W., "Numerical Solution of the Viscous Shock Layer Equations for Flow Past Spheres and Paraboloids," Final Rept., Contract 48-9195, Sandia Corporation.

[8] Blottner, F.G. and Flugge Lotz, I., "Finite Difference Computation of the Boundary Layer with Displacement Thickness Interaction," *Journal de Mecanque*, Vol. II, April 1963, pp. 397-423.

[9] Srivastava, B.N., Werle, M.J., and Davis, R.T., "Solution of the Hypersonic Viscous Shock Layer Equations for Flow Past a Paraboloid," Rept. AFL-74-4-10, 1974, Department of Aerospace Engineering, University of Cincinnati, Cincinnati, Ohio.

[10] Van Dyke, M., "Second Order Boundary-Layer Theory with Application to Blunt Bodies in Hypersonic Flow," AFOSR-TN-61-1270, 1961, Stanford University, Air Force Office of Scientific Research.

[11] Ferri, A., Zakkay, V., and Ting, L., "Blunt Body Heat Transfer at Hypersonic Speed and Low Reynolds Numbers," *Journal of Aerospace Sciences*, Vol. 28, Dec. 1961, pp. 962-971.

[12] Hickman, R.S. and Giedt, W.H., "Heat Transfer to a Hemisphere-Cylinder at Low Reynolds Numbers," *AIAA Journal*, Vol. 1, March 1963, pp. 665-672.

[13] Srivastava, B.N., Werle, M.J., and Davis, R.T., "Stagnation Point Solution of Viscous Shock Layer Equations for Flow Past a Sphere," Department of Aerospace Engineering, University of Cincinnati, Cincinnati, Ohio (in preparation).

[14] Russel, D.A., "Density Ahead of Sphere in Rarefield Supersonic Flow," *The Physics of Fluids*, Vol. 11, Aug. 1968, pp. 1679-1685.

[15] Jain, A.C. and Adimurthy, V., "Hypersonic Merged Stagnation Shock Layers, Part II, Cold Wall Case," *AIAA Journal*, Vol. 12, March 1974, pp. 348-354.
[16] Ahouse, D.R. and Bogdonoff, S.M., "An Experimental Flow Field Study of the Rarefied Blunt Body Problem," AIAA Paper 69-656, 1969, San Francisco, Calif.
[17] Li, C.P., "Hypersonic Nonequilibrium Flow Past a Sphere at Low Reynolds Numbers," AIAA Paper 74-173, Feb. 1974, Washington, D.C.
[18] Wittliff, C.E. and Wilson, M.R., "Low-Density Stagnation-Point Heat Transfer in the Hypersonic Shock Tunnels," *ARS Journal*, Vol. 32, 1962, pp. 275-276.
[19] Potter, L.J. and Miller, J.T., "Total Heating Load on Blunt Axisymmetric Bodies in Low Density Flow," *AIAA Journal*, Vol. 1, 1963, pp. 480-481.

Structural Optimization under Combined Blast and Acoustic Loading

S.S. Rao*
Indian Institute of Technology, Kanpur-16, India

Introduction

CONSIDERABLE amount of work has been reported in the literature on the minimum weight design of structures subjected to static and dynamic response restrictions.[1] The optimization of structures in a random vibration environment was discussed in Ref. 2. The minimum cost design of structures with random material properties has also been considered.[3] The present Note deals with the optimum design of beam-type and plate-type structures subjected to a constraint on the probability of failure due to combined blast and finite-duration acoustic loading. The present problem has application in the design of structures located near rocket testing or launching facilities where the structures may occasionally be exposed to blast loads due to explosions in addition to experiencing rocket-noise excitation. The expressions for the first passage probabilities of a linear oscillator are used in determining the damage probability of the given structure. The optimization problem is stated as a constrained nonlinear programing problem. The design of a simply supported rectangular plate is considered as an example problem.

Optimization Problem

The problem of optimum design of a structure subjected to combined blast and acoustic loading can be stated as a standard nonlinear programing problem as

Find $\boldsymbol{D}$ such that $f(\boldsymbol{D})\rightarrow$ minimum and $g_j(\boldsymbol{D})\leq 0, j=1,2,\ldots,m$

where $\boldsymbol{D}$ is the vector of design variables, $f(\boldsymbol{D})$ is the objective function and $g_j(\boldsymbol{D})$ are the constraint functions. The objective of the present work is to minimize the weight, and the major behavior constraint is that the probability of failure under the stated loading condition must be less than or equal to a specified value. The other constraints considered in this work include upper and lower limits on the fundamental natural frequency of the structure, upper and lower bounds on the design variables, and an upper bound on the time interval (T_c) required for the response autocorrelation function of the structure to decay to a small value. While the constraints on the fundamental frequency and the design variables are common for any dynamic structural optimization problem, the constraint on T_c becomes necessary in the present problem in view of the relations used for the failure probability of the structure.

Probability of Failure

It is well established that the stresses and deformations associated with the fundamental flexural modes of beam-like and plate-like structures exposed to acoustic pressures generally predominate over those associated with the higher modes. Thus an engineering estimate of the probability of failure can be obtained by idealizing the structure as a single degree-of-freedom oscillator corresponding to its fundamental mode.

Probability of Failure due to Individual Loads

The pressure vs time curves corresponding to blast loads generally rise very sharply and decay slowly. The displacement response $z(t)$ of a single degree-of-freedom oscillator to an exponentially decaying blast load $F_0\cdot e^{-\beta t}$ is given by

$$\frac{z(t)}{z_s}\left[\left(\frac{\beta}{\omega}\right)^2-2\zeta\frac{\beta}{\omega}+1\right]$$
$$=\left[\frac{\beta-\zeta\omega}{\omega(1-\zeta^2)^{1/2}}\right]e^{-\zeta\omega t}\cdot\sin\omega\sqrt{(1-\zeta^2)}\,t$$
$$-e^{-\zeta\omega t}\cdot\cos\omega(1-\zeta^2)^{1/2}t+e^{-\beta t} \qquad (1)$$

where $\omega=(K/M)^{1/2}=$ circular natural frequency of the oscillator, $K=$stiffness, $M=$mass, $z_s=(F_0/K)=$static deflection under a force F_0, $\beta=$decay exponent, and $t=$time. Equation (1) assumes that the oscillator is at rest and equilibrium at $t=0$. Thus, if the oscillator (structure) is excited by a blast load only, failure will occur if the maximum value of $z(t)$ given by Eq. (1) exceeds the prescribed limit Z in the time interval T.

If the structure is exposed to acoustic excitation only, the probability of failure in a time interval T can be calculated by considering the problem as a first passage problem.[4] In the present work, the random acoustic excitation and hence the response is assumed to be a Gaussian random process. Then the probability P that the absolute value of the displacement of a linear oscillator will exceed a threshold value Z in a time interval T is approximately given by[4]

$$P[\,|z(t)|>Z]=P(Z,T)=1-Ae^{-\alpha fT} \qquad (2)$$

where f is the natural frequency of the oscillator, and A and α are functions of the threshold level Z, the conditions of motion at the beginning of the time interval T, and the damping of the oscillator. The values of A and α can be obtained for any specified Z.[4] It is to be noted that Eq. (2) holds true for time intervals $T>T_c$, where T_c denotes the time interval required for the response autocorrelation function to decay to a small value. The expression for T_c may be taken as

$$T_c\simeq 1/(2\pi f\zeta) \qquad (3)$$

where ζ is the damping ratio of the oscillator.

Probability of Failure When Both Loads Act Simultaneously

It can be seen that for a slowly decaying force ($\beta/\omega<<1$) and for an oscillator with negligible damping, Eq. (1) may be approximated as

$$[z(t)/z_s]\,[1+(\beta/\omega)^2]=1-\cos\omega t \qquad (4)$$

On the other hand, for a rapidly decaying force ($\beta/\omega>>1$), Eq. (1) becomes

$$[z(t)/z_s]\,[1+(\beta/\omega)^2]=(\beta/\omega)\sin\omega t \qquad (5)$$

Received July 28, 1975.
Index category: Structural Design, Optimal.
*Assistant Professor, Department of Mechanial Engineering.